

# *Positioning Control of One Link Arm with Parametric Uncertainty using Quantitative Feedback Theory*

Takayuki KUWASHIMA \* , Jun IMAI and Masami KONISHI

Dept. of Electrical and Electronic Engineering

Okayama University

3-1-1, Tsushima-Naka Okayama, 700-8530

(Received November 21, 2008)

This paper presents method of the controller design for one link arm with parametric uncertainty. Recently, many manufacturing robots are operated in manufacturing facilities, with the aim of labor and cost saving or improvement of the productivity. Such robots need to have positioning performance of high precision. In condition that there is an uncertainty in plant dynamics, desired control performance may not be attained because the controller is designed according to the mathematical model of a plant. So it is important that the designed control system have a robust control performance. In this paper, the robust controller is designed using Quantitative Feedback Theory (QFT) for one link arm with parametric uncertainty. Simulation experiments are run for control system designed by using QFT and conventional method. The results are compared with each other and it is found that the control system designed by QFT shows a robust performance and can suppress the unevenness of output against parametric uncertainty.

## 1 INTRODUCTION

Recently, many manufacturing robots are operated in manufacturing facilities, with the aim of labor and cost saving or improvement of the productivity. In particular, automatic sorting robots for products in assortment line are used to improve the productivity. In case of having the robots do such operations, it is demanded that they have manipulator tip positioning performance of high precision to the target position. But in condition that products of various weights are handled, positioning precision and control performance, such as settling time, would deteriorate because controller are designed according to the mathematical models that represent these dynamics, and they include parameters, such as weights of grabbing product with the robot hand. So the controller needs to have

robust control performance against parameter uncertainty in the plant dynamics. It means that control system maintain its performance constant even if there is a parametric uncertainty. Recently, many studies for control problem under plant uncertainty are done because conventional control theory is based on the assumption that the dynamics of plant is well-known, and that the mathematical model of controlled object accurately reflects behavior of that in the real world. Nowadays, robust control theory is developed in order to solve these problems and H infinity control theory, one of robust control theories, is applied to many control systems. H infinity control theory can handle unstructured uncertainty of the plant, but it can not directly cope with structured uncertainty such as parameter variations. It is not perfect that the control performance can not be guaranteed.

---

\*E-mail: kuwashima@cntr.elec.okayama-u.ac.jp

In this paper, Quantitative Feedback Theory [1] (QFT) is introduced and robust controller for one link arm with parametric uncertainty is designed by using it. QFT is one of the robust control theories, and can cope with parametric uncertainty in a plant. So QFT is applied to robust control in recent research[2],[3]. In design procedure, the area where plant can exist in accordance with parameter variation is illustrated on Nichols chart for each frequency. It is called template. By using it, the controller is designed in order to satisfy performance specification for plants.

## 2 PROBLEM DESCRIPTION

The object of this research is one link arm as shown in Fig.1. It simulates the sorting robot in manufacturing facility. It consists of a Direct-Drive (DD) motor as an actuator, a rigid arm and a payload mass at free end of arm, imitating carried product. The arm is driven by DD motor and rotates in the horizontal plane. DD motor is actuated by input torque  $\tau$ [Nm]. The specification of motor is as shown in Table.1. The arm is made of aluminum with length of  $L=0.3$ [m].

This time, we consider 4 kinds of product, it's weights are as follows.

$$M = 0.8, 1.6 \ 2.4 \ 3.2[\text{kg}] \quad (1)$$

This imitates the condition that the robot grasps loads of different weights.

Control objective is to control angular position of this arm from the initial position to the target position. To realize positioning control, angular position feedback control is applied.

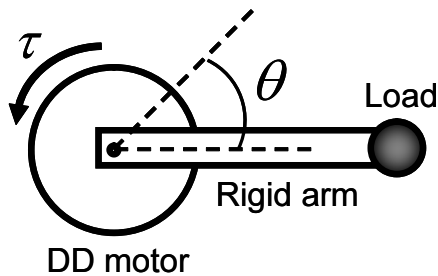


Fig. 1 One link arm

Table. 1 Specification of DD motor

Rated voltage[V]	200
Rated torque[N·m]	25
Rated current[A]	2.7
Rated velocity[ $\text{min}^{-1}$ ]	150
Inertia moment $J_0$ [ $\text{kg}\cdot\text{m}^2$ ]	0.0909

## 3 MODELING OF ONE LINK ARM

### 3.1 Mathematical Model

Let  $\theta(t)$  be the angle of rotation from the initial position, the dynamics equation describing this system is expressed by the following equation.

$$J\ddot{\theta} + D\dot{\theta} = \tau \quad (2)$$

The Laplace transform of Eq.(2) gives the transfer function from  $\tau$  to  $\theta$  as follows;

$$P(s) = \frac{1}{Js^2 + Ds} \quad (3)$$

Here,  $J$  donates rotating inertia of whole arm system, and is represented as follows;

$$J = J_0 + \frac{\rho L^3}{3} + ML^3 \quad (4)$$

$D$  is the friction coefficient around the motor rotary axis. From Eq.(4), it is found that value of  $J$  varies depending on weight of product. This time, we consider 4 kinds of product, it's weights are 0.8 to 3.2 at 0.8[kg] intervals.

### 3.2 Parameter Observation

In order to get the values of 2 parameters at each load, observation experiment of these parameters using correlation method has been run .

#### 3.2.1 Correlation Method

Correlation method is one of the system identification techniques. The feature of correlation method is that this method is not affected by noise or disturbance. In this method, the observed data is subjected to signal process and noise or disturbance on the data are rejected.

Consider sin wave signal  $u(t) = A \sin \omega t$  as input signal to identified object  $G(j\omega)$ , stationary response of output is as follows.

$$y(t) = B_1 \sin(\omega t + \theta_1) + \sum_{k=2}^{\infty} B_k \sin(k\omega t + \theta_k) + v(t) \quad (5)$$

Here, the first item of right hand side of Eq. donates the frequency response to be estimated, the second part means high frequency component,  $v(t)$  represents disturbance noise. By multiplying  $y(t)$  by  $\sin \omega t$  and  $\cos \omega t$ , and calculating a cycle average, we get  $U$  and  $U'$  as follows.

$$U = \frac{1}{T} \int_0^T y(t) \sin \omega t \cdot dt \simeq \frac{B_1}{2} \cos \theta_1 \quad (6)$$

$$U' = \frac{1}{T} \int_0^T y(t) \cos \omega t \cdot dt \simeq \frac{B_1}{2} \sin \theta_1 \quad (7)$$

where  $T = 2n\pi/\omega$

Then, the gain and phase date of  $G(j\omega)$  at  $\omega$  are obtained as follows.

$$|G(j\omega)| = \frac{B_1}{A} \simeq \frac{2}{A} \sqrt{U^2 + U'^2} \quad (8)$$

$$\arg G(j\omega) = \theta_1 \simeq \tan^{-1}(U'/U) \quad (9)$$

### 3.2.2 Observation Experiment

This time, transfer function from input torque to rotary velocity,  $P_w(s)$ , is used as identified object.

$$P_w(s) = \frac{1}{Js + D} \quad (10)$$

Firstly, rotary velocity response for sinusoidal input torque is measured. Then, signal process of Eq.6 to Eq.9 are applied to rotary velocity response and the gain and phase date without disturbance noise are obtained. Finally, least squares method are applied to get the values of  $J$  and  $D$ .

Measurement date and fitting curves of frequency response of  $P_w$  are shown in Fig.2. The values of  $J$  and  $D$  are shown in Table.

From observation experiment, the range of vary in  $J$  and  $D$  are obtained as follows;

$$J \in (0.0435, 0.2046), D \in (0.1741, 0.1852) \quad (11)$$

## 4 SYSTEM DESIGN USING QFT

In this section, control system design using QFT is mentioned.

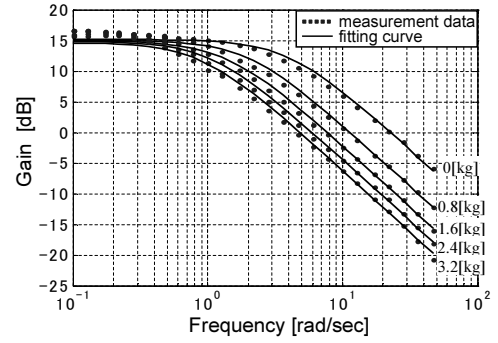


Fig. 2 Frequency response of  $P_w$  at each load

Table. 2 Estimation result of  $J$  and  $D$

	$J[\text{kg} \cdot \text{m}^2]$	$D[\text{N} \cdot \text{m} \cdot \text{s}]$
0[kg]	0.0435	0.1741
0.8[kg]	0.0870	0.1766
1.6[kg]	0.1285	0.1791
2.4[kg]	0.1661	0.1807
3.2[kg]	0.2046	0.1852

### 4.1 Overview of QFT

QFT is one of the robust design techniques and based on loop shaping method on Nichols chart. The remarkable future of QFT is that QFT method can cope with parametric uncertainty in plant. If there is parametric uncertainty in plant, response of plant may varies like Fig.3. The goal of design with QFT is to suppress unevenness of plant response and put them between performance specs which represents desired response, as shown in Fig.3.

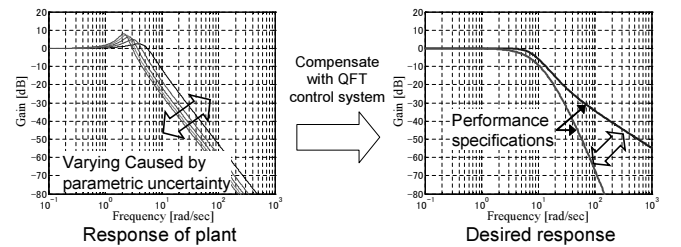


Fig. 3 Overview of QFT

In QFT design procedure, designer determines the performance specifications that response of plant should lie in. It has certain width as tolerance in time and frequency domains. Controller is designed on Nichols Chart (NC) so that all responses of plant lie between

these specifications. The indices to meet these specifications are described on NC as boundary, and used in controller design on NC.

Consider feedback control system shown in Fig.4. We design  $C(s)$  and  $F(s)$  in order to satisfy performance specifications. The key points of design with QFT are following;

- limit the maximum peak gain of closed loop transfer function  $T(s)$
- narrow the fluctuation of  $T(s)$
- set the position of  $T(s)$  between performance specifications

QFT design procedure is as follows;

**STEP1** Determine performance specification in time and frequency domains.

**STEP2** Gain the area where varying plant can exist on NC, called template.

**STEP3** Construct performance specification on NC as bounds.

**STEP4** Form the open loop transfer function  $L(s) = C(s)P(s)$  to satisfy bounds.

**STEP5** Design the filter  $F(s)$ .

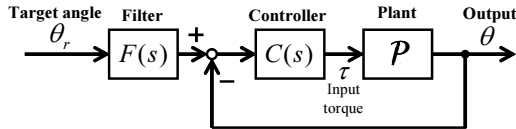


Fig. 4 QFT Control System

## 4.2 Performance Specification

Here, performance specifications in time domain are determined as follows;

$$\text{Overshoot : } O_s = 0 \sim 5\% \quad (12)$$

$$\text{Settling time : } t_s < 1.0[\text{sec}] \quad (13)$$

$$\text{Peak gain : } M_p < 1.2 \quad (14)$$

In QFT, more concrete specification is constructed so as to have certain width by determining upper and lower bounds according to Eqs.12 and 13. Transfer functions  $T_{RU}$ ,  $T_{RL}$ , that represent upper and lower

bounds respectively, are designed such as following equations. The time and frequency responses of these functions have forms as shown in Figs.5 and 6.

$$T_{RU}(s) = \frac{1.83(s + 30)}{s^2 + 10.5s + 54.8} \quad (15)$$

$$T_{RL}(s) = \frac{5 \times 10^4}{(s + 50)(s + 10)^3} \quad (16)$$

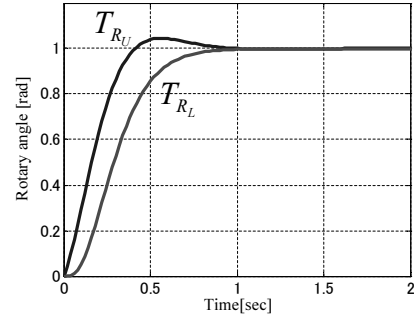


Fig. 5 Performance Specification (Time domain)

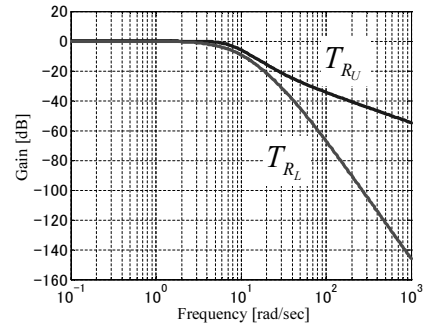


Fig. 6 Performance Specification (Frequency domain)

## 4.3 Template

One of the features of QFT is to describe the plant as a contour on NC. The plant without parameter uncertainty is expressed as single point at certain frequency on NC. If there is variation in parameter of plant, the plant is expressed on NC as contour for each value of frequency. It is referred to as a *template*. Therefore template represents the region where the varying plant can exist. So the designer can confirm uncertainty in plant visually from templates.

From observation experiment in previous section, the range of vary in  $J$  and  $D$  are  $J \in (0.0435, 0.2046)$ ,  $D \in$

(0.1741, 0.1852). The variation range of these parameters is described as Fig.7. Consider 6 points on the variation range as an example, the template at 2[rad/sec] has form as shown in Fig.8. This template shows the area where  $P(s)$  can exist at 2[rad/sec]. In actual design process, we consider 20 points on the variation range.

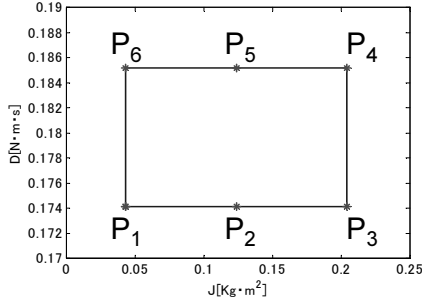


Fig. 7 Variation range of  $J$  and  $D$

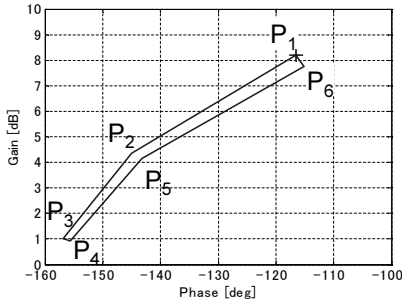


Fig. 8 Template at 2[rad/sec]

Fig.9 shows templates of  $P(s)$  with variations of  $J$  and  $D$  at each frequency.

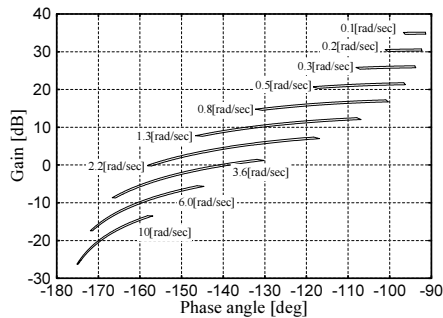


Fig. 9 Template of  $P(s)$  at each frequency

## 4.4 Bounds on NC

In QFT design process, bounds are constructed on NC, that represent condition for control system to meet the preformance specifications. There are 2 kinds of bounds, U-contour and  $B_R$  bounds. There are used in loop shaping process of open loop transfer function as indices.

### 4.4.1 U-contour

U-contour is constructed on NC and represents the condition to attenuate the peak gain of the closed loop transfer function below certain value. It is represented by a closed curve. If the gain-phase curve of open loop  $L(s)$  doesn't break into U-contour, performance specification about peak gain will be met. Detail of construction of U-contour is described below.

Assume that performance specification about the peak gain of closed loop  $T(s)$  is as follows.

$$|T(s)| < M_p \quad (17)$$

This equation establishes a circle of constant  $M_p$ , called M-contour (See Appendix). On the condition that there is no parameter variation in  $P(s)$ , the peak gain of  $T(s)$  will be below  $M_p$  when the gain-phase curve of  $L(s)$  doesn't break into M-contour of  $M_p$ , according to the characteristic of NC. On the other hand, if there is parameter variation in  $P(s)$ , the gain-phase curve has some fluctuation and be expressed as templates at each frequency, as described previously. So some templates can interfere in M-contour, even if the gain-phase curve is outside of it or tangent to it. To solve the problem, consider having M-contour some gain margin

Suppose that the maximum variation range of all template is  $V$ [dB]. Let the lower half part of M-contour be translated vertically by  $V$ [dB]. This closed curve is called U-contour. If the gain-phase curve is outside of U-contour or tangent to it, Eq.17 will be met for all varying  $P(s)$  because the gain margin of  $V$ [dB] are taken into account. This time, value of  $M_p$  and  $V$  are as follows. In case of that, U-contour has the form as shown in Fig.10.

$$M_p = 1.2, \quad V = 13.4[\text{dB}] \quad (18)$$

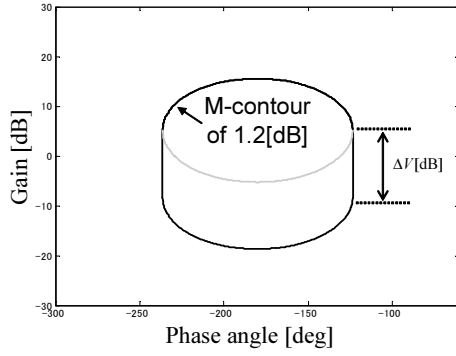


Fig. 10 U-contour

#### 4.4.2 $B_R$ Bounds

$B_R$  Bounds are constructed on NC and expressed as open curve. It represents the condition for the fluctuation range of closed loop  $T(s)$  to be narrow than the range between the upper and lower performance specifications. And it is obtained at each frequency. If the position of the gain-phase curve at certain frequency,  $L(j\omega)$ , is above or on the corresponding  $B_R$  Bound, the fluctuation range will be suppressed. Detail of construction of  $B_R$  Bounds is described below.

In order for closed loop  $T(s)$  to lie between upper and lower performance specifications, the following condition about their fluctuation range at each frequency should be met.

$$\delta_L(j\omega_i) \leq \delta_R(j\omega_i) = 20 \log_{10} |T_{RU}(j\omega_i)| - 20 \log_{10} |T_{RL}(j\omega_i)| \quad (19)$$

Now, let us consider the fluctuation on NC. As mentioned previously, the template represents the spread of gain-phase curve of open loop  $L(s)$ , induced by parameter variation of  $P(s)$ , at each frequency on NC. On the other hand, the information of the gain of  $T(s)$  is obtained once the gain-phase curve of  $L(s)$  is plotted, according to the characteristic of NC. So the fluctuation ranges of  $T(s)$  at each frequency are caught from templates on NC. For example, the template at  $\omega=2[\text{rad/sec}]$  is shown in Fig.11. From this Figure, it is known that the template is tangent to M-contours of  $M=8.1[\text{dB}]$  and  $0.87[\text{dB}]$ . This means that the maximum gain of  $T(s)$  at  $2[\text{rad/sec}]$  is  $8.1[\text{dB}]$  and the minimum gain is  $0.87[\text{dB}]$ . So the fluctuation ranges of  $T(s)$  at  $2[\text{rad/sec}]$ ,  $\delta_L(j2)$ , is obtained to be  $8.1-0.87=7.2[\text{dB}]$ . In contrast, the allowable range  $\delta_R(j2)$  is known from upper and lower specifications to be

$0.51[\text{dB}]$ . It is found that  $\delta_L$  isn't lower than  $\delta_R$  without compensation. In order to meet Eq.20, the open loop transfer function should be compensated with  $C(s)$  as follows.

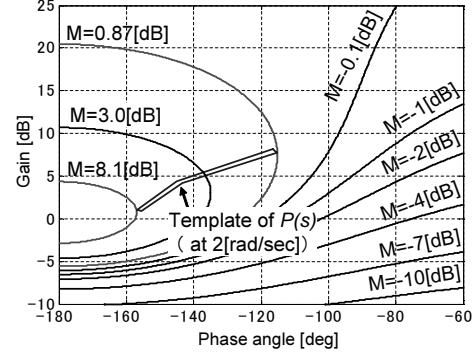


Fig. 11 Template at 2[rad/sec] and M-contours

$$L(s) = C(s)P(s) \quad (20)$$

This equation can be divided into 2 equations about gain and phase angle.

$$20 \log_{10} |L(s)| = 20 \log_{10} |C(s)| + 20 \log_{10} |P(s)| \quad (21)$$

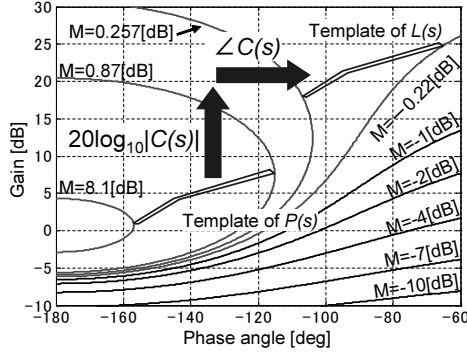
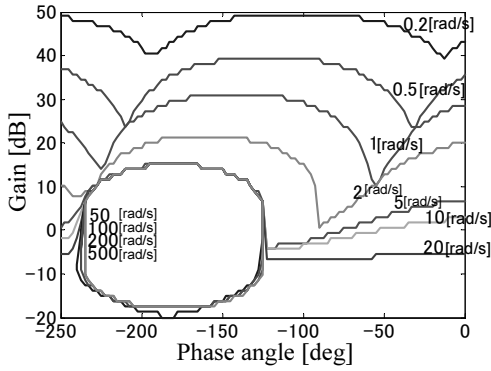
$$\angle L(s) = \angle C(s) + \angle P(s) \quad (22)$$

Therefore, the template of  $P(s)$  can be converted into the template of  $L(s)$  by translating it vertically by  $20 \log_{10} |C(s)|[\text{dB}]$ , and horizontally by  $\angle C(s)[\text{deg}]$ . Fig.12 shows the case of translating by  $17[\text{dB}]$  and  $50[\text{deg}]$ . From this figure, it is found that the template of  $L(s)$  is tangent to M-contours of  $M=0.257[\text{db}]$  and  $-0.22[\text{db}]$ , and that  $\delta_L(j2)$  is obtained to be  $0.257-(-0.22)=0.479[\text{db}]$ . So this case satisfies Eq.20. On the other hand,  $\delta_L(j2)$  in the case of translating by  $16.32[\text{dB}]$  is found to be  $0.51[\text{dB}]$  and this place becomes the limiting point to meet Eq.20. Thus the limiting points to meet Eq.20 can be obtained at each value of  $\angle C(s)$ , and the bound can be obtained by connecting these points. The group of the bounds that are obtained at each frequency are called  $B_R$  bounds. In designing process of  $C(s)$ ,  $C(s)$  should be determined so that the place of the gain-phase curve of  $L(s)$  at each frequency is on or above the corresponding  $B_R$  bound.

$B_R$  Bounds and U-contour are shown in Fig.13

#### 4.5 Form of Open Loop $L(s)$

In former section, the indices to meet performance specification have been constructed. Next, the open

Fig. 12 Template of  $L(s)$  at 2[rad/sec] and M-contoursFig. 13 U-contour and  $B_R$  bounds

loop transfer function  $L(s)$  will undergo a loop shaping by synthesizing  $C(s)$ .<sup>97.1</sup> This time, PID compensator is applied as  $C(s)$ . The design principles are as follows.

- Not to break into U-contour
- To be on or above the  $B_R$  Bounds at each frequency

The form of designed  $C(s)$  is following.

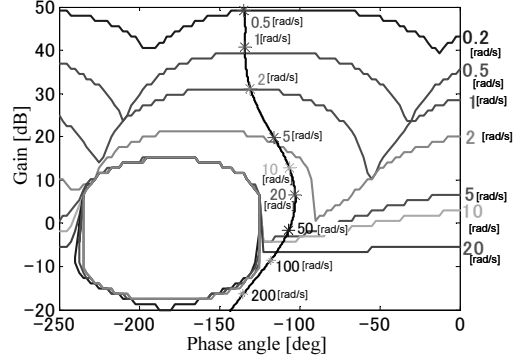
$$C(s) = K_P + \frac{K_I}{s} + \frac{K_D s}{T_D s + 1} \quad (23)$$

$$K_P = 28, K_I = 5.6, K_D = 8.4, T_D = 0.005 \quad (24)$$

The gain-phase curve of  $L(s)$  using  $C(s)$  of Eq.23 and Bounds are shown in Fig.14. From this figure, the gain-phase curve meets bounds at each frequency.

#### 4.6 Synthesis of $F(s)$

In previous part, the loop shape of the open loop  $L(s) = C(s)P(s)$  has been done, and the fluctuation range of the closed loop  $T(s)$  has been narrowed so

Fig. 14 The gain-phase curve of  $L(s)$  and Bounds

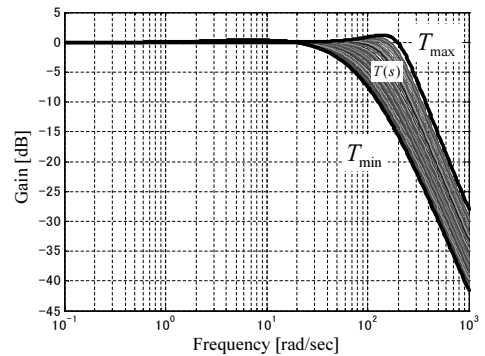
that Eq.20 is met. Here the transfer function of  $T(s)$  is expressed as follows.

$$T(s) = \frac{L(s)}{1 + L(s)} \quad (25)$$

But there is no guarantee that the frequency response of  $T(s)$  lies between upper and lower performance specifications. Thus consider shaping of the frequency response of entire control system  $T_R(s)$  and positioning them between upper and lower specifications, by synthesizing the filter  $F(s)$  and inserting it in front of  $T(s)$  as shown in Fig.4. The transfer function of  $T_R(s)$  is expressed as follows.

$$T_R(s) = F(s) \frac{L(s)}{1 + L(s)} = F(s)T(s) \quad (26)$$

The frequency responses of  $T(s)$  are shown in Fig.15.

Fig. 15 The frequency response of  $T(s)$ 

From these responses, the bounds representing the maximum gain  $T_{\max}$ , and the minimum gain  $T_{\min}$  are obtained. Next, plot the graph which is expressed by the

following equations.

$$20 \log_{10} |T_{R_U}| - 20 \log_{10} |T_{\max}| \text{ vs } \omega \quad (27)$$

$$20 \log_{10} |T_{R_L}| - 20 \log_{10} |T_{\min}| \text{ vs } \omega \quad (28)$$

$$(29)$$

This graph is shown in Fig.16. These 2 lines form

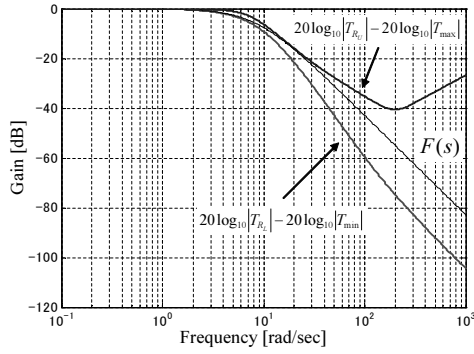


Fig. 16 The frequency response of  $F(s)$

a certain range. By synthesizing  $F(s)$  in order to lie between this area, the frequency response of  $T_R(s)$  can lie between performance specifications. Designed  $F(s)$  has form as follows.

$$F(s) = \frac{1}{(s+8)(s+9)} \quad (30)$$

The frequency response of  $T_R(s)$  using this  $F(s)$  is shown in Fig.17. From this figure, the fluctuation of  $T_R(s)$  caused by the variation of  $P(s)$  is suppressed, and the responses of  $T_R(s)$  lie between upper and lower performance specifications.

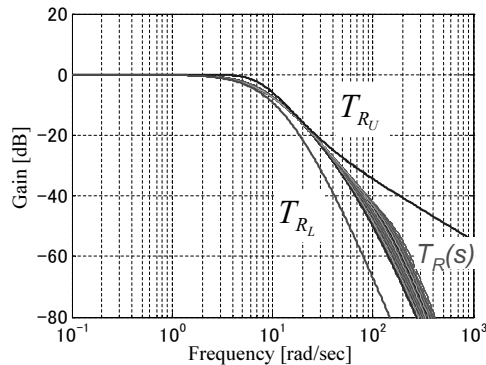


Fig. 17 The frequency response of  $T_R(s)$ ,  $T_{R_U}(s)$  and  $T_{R_L}(s)$

## 5 EXPERIMENT

This section shows description of the experimental system and experimental result.

### 5.1 Experimental System

Experimental test has been done on the actual system to verify the effectiveness of designed controller. Detail of experimental system is described below.

Fig.18 shows the actual one link arm used in experiment. It contains DD motor SGMCS – 25D produced by YASKAWA Electric Corporation. Specification of motor is shown in Tab.1. Fig.19 shows general figure of experimental system. The block diagram for control is constructed on SIMULINK, which is the application software of MATLAB produced by The MathWorks, Inc. The block diagram is converted into C-code by MATLAB's tool, Real-Time-Workshop, and loaded on DSP board DS1104 produced by dSPACE GmbH. This system can mount the same control system as the block diagram.

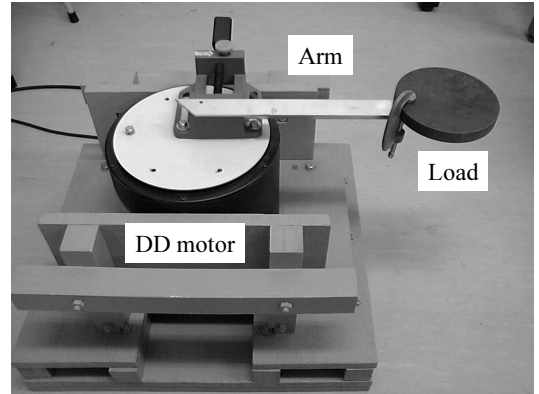


Fig. 18 One link arm

### 5.2 Experimental Result

As a comparison method, PID controller is applied which is used generically for various applications. Controller gain has been determined by adjustment on actual one link arm system. The controller has form as follows.

$$C(s) = 4 + \frac{0.5}{s} + \frac{s}{0.1s+1} \quad (31)$$

$$F(s) = \frac{1}{0.15s+1} \quad (32)$$



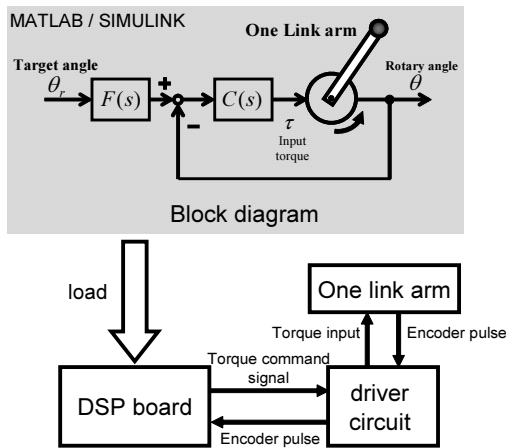


Fig. 19 Experimental system

Each control system has been mounted on experimental system, and experiment has been done. As the reference signal, square wave of amplitude of  $\pm 20$ [deg] and a period of 10[sec] is used. Control cycle is 1[msec]. The experimental result in condition of using 5 pattern of load weight are shown in Figs.20,21. From Fig.20, it is found that control performance is affected due to variation of weight of load in conventional method. On the other hand, control system designed by QFT is not affected in spite of load variation. From these result, robust control system can be realized by designing with QFT.

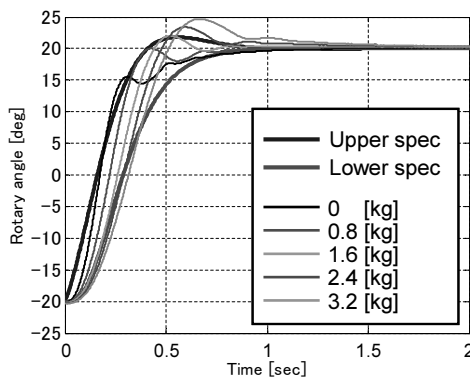


Fig. 20 Control result with PID

## 6 CONCLUSION

In this paper, QFT method has been successfully applied to the one link arm system and robust control system has been designed. In this method, con-

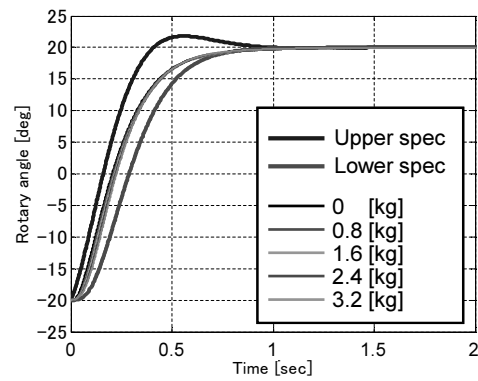


Fig. 21 Control result with QFT

troller is designed so that the frequency response of the control system lies between performance specifications that represent desired response. The indices which are used in design procedure are constructed on NC by using templates which represent a uncertainty in the transfer function of one link arm. Experiment has been performed using actual one link arm system and control performance has been tested experimentally. Through experimental test, it shows robust control performance against parameter uncertainty, compared with conventional PID control method. In future works, conventional robust control theory will be applied, and compared with QFT.

## REFERENCES

- [1] Constantine H. Houppis, Quantitative Feedback Theory Fundamentals and Applications, *Taylor & Francis*, (2005), 22-99.
- [2] A. Khodabakhshian, N. Golbon, Proc. 13th Mediterranean Conference on Control and Automation, Limassol, Cyprus, (2005), 970-975.
- [3] J. J. Barve and P.S.V. Nataraj, Intl. Conf. TENCON-98 IEEE R-10, New Delhi, (1998).
- [4] Humiharu Kondo, Basic Control Engineering (In Japanese), Morikita syuppan, (1998), 94-96.
- [5] Araki Mituhiko, Classic Control Theory (In Japanese), Baifukan, (2000).

## APPENDIX

Nichols chart shows the link between the gain and phase angle of open loop and closed loop system.

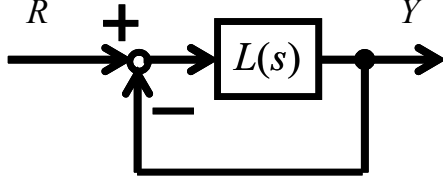


Fig. 22 Unity Feedback System

Consider the unity feedback system shown in Fig.22. Let  $L(s)$  be the open loop transfer function, then the closed loop transfer function  $T(s)$  is expressed in the following equation

$$T(s) = \frac{L(s)}{1 + L(s)} \quad (33)$$

Here, let  $L(s)$  and  $T(s)$  to be expressed as following equations where  $s = j\omega$ .

$$L(j\omega) = c \exp(j\theta) \quad (34)$$

$$T(j\omega) = M \exp(j\alpha) \quad (35)$$

So the gain  $M$  and the phase angle  $\alpha$  of frequency response of  $T(s)$  are obtained as follows.

$$M = \left\{ \left( \frac{1}{c} + \cos \theta \right)^2 + \sin^2 \theta \right\}^{-1/2} \quad (36)$$

$$\alpha = \tan^{-1} \left( \frac{\sin \theta}{c + \sin \theta} \right) \quad (37)$$

The gain-phase curve of open transfer function  $L(s)$  is plotted on the gain-phase plain, which takes gain in dB on vertical axis and phase angle in degrees on horizontal axis. By using Eq.36 and 37, value of  $M$  and  $\alpha$  are determined uniquely against single point on gain-phase curve of  $L(s)$ . Therefore, the curve of constant value of Eq.36, called M-contour, and the curve of constant value of Eq.37, called  $\alpha$ -contour, can be plotted on the gain-phase plain for each value of gain and phase of  $L(s)$ . Once the gain-phase curve of  $L(s)$  is plotted, the gain and phase of  $T(s)$  can be obtained from the graph. The gain-phase graph which is superimposed on the graph with M-contours and  $\alpha$ -contour is called Nichols Chart [4][5]. M-contour has the characteristic that M contour forms a circle surrounding a point of (0[dB], -180[deg]) in case of  $M > 0$ , and M contour forms a curve in case of  $M < 0$ . Additionally the lower the diameter of M contour is, the higher the value of  $M$  becomes. It means the gain of the closed loop system increases.

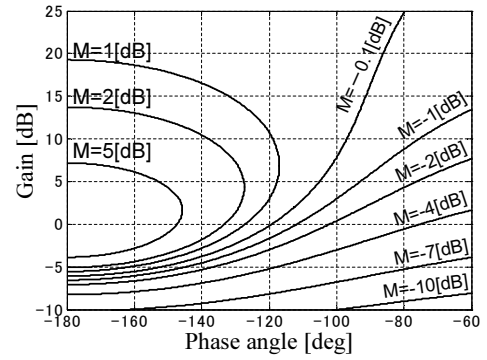


Fig. 23 M contours